Seitz, F., M. Schmidt, C.K. Shum: Signals of extreme weather conditions in Central Europe from GRACE 4-D hydrological mass variations. Earth and Planetary Science Letters, 268(1-2), 165-170, 2008.

DOI: 10.1016/j.epsl.2008.01.001

Signals of Extreme Weather Conditions in Central Europe in GRACE 4-D Hydrological Mass Variations

Florian Seitz [a,*],

[a] *Earth Oriented Space Science and Technology (ESPACE), Technische Universität München, Arcisstr. 21, 80333 Munich, Germany.*

Michael Schmidt [b]

[b] *Deutsches Geodätisches Forschungsinstitut (DGFI), Marstallplatz 8, 80539 Munich, Germany*

C.K. Shum [c]

[c] *Geodetic Science, School of Earth Sciences, The Ohio State University, Columbus, U.S.A.*

Abstract

We report evidence of observed extreme weather fluctuations in Central Europe by satellite gravimetry during the last five years. Heat waves, droughts, excessive rain, snowfall, and floodings occurred frequently during the study period. Such phenomena are primarily associated with hydrological mass variations that are manifested in the changes of the Earth's gravity field, sensitive to the Ka-band satellite-to-satellite ranging (KBR) measurements onboard of the gravity field mission GRACE twin-satellites 2002-2007. In our contribution we perform a regional analysis of GRACE data over Europe based on spherical wavelet/B-spline and global spherical harmonic solutions. Resulting temporal gravity field variations are expressed in terms of equivalent water mass variations which are subsequently compared and in balance with the net effect of precipitation and evaporation from the atmospheric flux convergence reduced by runoff from river gauge data for seven Central European river basins.

Key words: GRACE, gravity field variations, continental hydrology, atmospheric moisture budget
PACS: 91.10.Op, 92.40.qp, 92.60.J

* Corresponding author. Tel: +49-89-28923-184, Fax: +49-89-28923-178
Email address: `seitz@bv.tum.de` (Florian Seitz).

1 Introduction

Since March 2002 the satellite mission GRACE (Gravity Recovery and Climate Experiment) allows for the observation of spatial and temporal changes of the Earth's gravity field (Tapley et al., 2004) which are associated with the redistribution of masses within and between individual components of the Earth system. Due to its near-polar and low orbit GRACE allows for an almost global coverage of gravity field variations with an unprecedented spatial resolution of about 400-500 km (half-wavelength) and a temporal resolution of one month or shorter.

On hourly to seasonal time-scales the largest mass fluctuations in the Earth system are caused by lunisolar tides and dynamic processes within the atmosphere, the oceans, the cryosphere and the continental hydrosphere. Periodic mass redistributions at high frequencies due to, for example, rapid transient geophysical processes (e.g. from atmospheric pressure variations or oceanic circulation) would cause aliasing of the gravity estimates from GRACE if not treated accordingly. In particular, tides (solid Earth, ocean and pole tides) and non-tidal variations including the response of the solid Earth and ocean to pressure and wind forcing as well as the atmospheric aliasing effect are assumed known, and forward-modeled prior to the inversion of the GRACE monthly gravity field solutions (Flechtner, 2003; Schmidt et al., 2006). Consequently the largest part of the remaining gravity field variation signal over our study region in Central Europe reflects mass variations within the continental hydrosphere including snow and ice melt/accumulations (apart from measurement errors, deficiencies of the de-aliasing products and long-term variability of other components of the Earth system).

Observed gravity field changes are commonly expressed in terms of equivalent water height (EWH) variations. EHWs are an idealized representation of the causative mass variations, i.e., a measure for the thickness of a water layer that needs to be added to (or removed from) the Earth's surface if the total observed gravity field fluctuations would be due to the change of water storage. The global mean of the accuracy of the EWH estimates from GRACE is about 1-2 cm (Swenson et al., 2003; Wahr et al., 2006). Several analyses of water storage changes on global or regional scales have been performed (e.g., Schmidt et al., 2006; Swenson et al., 2006). Most of the studies are based on results using GRACE spherical harmonic solutions.

In this contribution we compare GRACE EWH estimates from different approaches, namely from two global spherical harmonic solutions and from our regional multi-resolution representation (MRR) based on spherical wavelets (Section 2). Our analyses are performed for a contiguous area of seven Central European river basins (Fig. 1, left) covering $1.46 \cdot 10^6$ km^2. GRACE observations of equivalent water mass changes in this region are compared with water storage estimates from the convergence of vertically integrated water vapor fluxes reduced by river discharge from gauge registrations (Section 3). The results are analyzed with respective to specific weather phenomena in Central Europe between 2002 and 2007 (Section 4).

FIGURE 1 HERE

2 Mass Variations from GRACE Gravity Field Observations

2.1 Regional GRACE 4-D Wavelet Expansion

In our spatio-temporal (4-D) wavelet approach we model the difference $\delta V(\boldsymbol{r}, t)$ ($\boldsymbol{r}$ = position vector, t = time) between the geopotential $V(\boldsymbol{r}, t)$ and a time-invariant reference model $V_{\text{ref}}(\boldsymbol{r}, t)$ (here: GGM01C) by the multi-resolution representation (MRR)

$$\delta V(\boldsymbol{r}, t) = \sum_{i=i'}^{I} v_{i;J_i}(\boldsymbol{r}, t) \tag{1}$$

(Schmidt et al., 2007, 2008). Herein each 4-D detail signal $v_{i;J_i}$ is related to a specific spatial frequency band B_i and a specific temporal frequency band B_{J_i}. Mathematically this statement can be expressed by the series expansion

$$v_{i;J_i}(\boldsymbol{r}, t) = \sum_k \sum_l d_{i,k;J_i,l}\, \psi_{i,k}(\boldsymbol{r})\, \phi_{J_i,l}(t) \ , \tag{2}$$

wherein the (spatial) level$-i$ spherical wavelets $\psi_{i,k}(\boldsymbol{r})$ act as band-pass filters and the (temporal) level$-J_i$ scaling functions $\phi_{J_i,l}(t)$ as low-pass filters. In our investigations we apply spherical Blackman wavelets $\psi_{i,k}$ (Schmidt et al., 2007) and quadratic B-spline scaling functions $\phi_{J_i,l}$ (Schmidt et al., 2008). The higher the level values J_i and i are chosen, the finer are the temporal resolution and the spatial structures of the gravity field that can be resolved. Due to the localization properties of wavelets the coefficients $d_{i,k;J_i,l}$ are estimable from regional gravity observations by least-squares techniques considering regularization strategies (Schmidt et al., 2007).

We processed the GRACE Level 1B data product via the energy balance approach to produce residual GRACE geopotential difference observations $\Delta V_{1,2}(t) = \delta V(\boldsymbol{r}_1(t), t) - \delta V(\boldsymbol{r}_2(t), t)$; $\boldsymbol{r}_1(t)$ and $\boldsymbol{r}_2(t)$ are the trajectories of the two GRACE satellites. Applying appropriate background models and correcting GRACE accelerometer biases and relative velocity and position vectors, we assume that $\Delta V_{1,2}$ primarily reflects hydrology variations (Han et al., 2006) in our study region. The data are available between September 2002 and July 2005, except for December 2002, January and June 2003, parts of January 2004 (orbit manoeuvers and data gaps) and the time span between August and November 2004 when GRACE almost entered a repeat orbit (Wagner et al., 2004). Following Farrell's theory (Farrell, 1972) the geopotential results are transformed into equivalent water heights; for more details see Schmidt et al. (2008).

2.2 Monthly mass grids from GRACE spherical harmonic solutions

Mass variations from global GRACE spherical harmonic solutions are derived from the latest releases RL04 from two of the GRACE data processing centers at GFZ (GeoForschungsZentrum Potsdam) and CSR (Center for Space Research, U. Texas). Chambers (2006) computed quasi-monthly global $1^\circ \times 1^\circ$ grids of EWH variations from the respective sets of spherical harmonic coefficients (Level 2 data products). The EWH grids are publicly available at http://grace.jpl.nasa.gov. At present (December 2007) the time spans between February 2003 and November 2006 (GFZ) and between August 2002 and December 2006 (CSR) are provided. Again the fields for June 2003 and January 2004 are missing in both data sets.

Large errors in the form of longitudal stripes are present in the current GRACE gravity field variations from Level 2 data products. They are primarily due to the satellite orbit characteristics and GRACE measurement limitations (KBR is along the twin-satellite orbital tracks which are primarily co-planar), which result in inability to separate spherical coefficients at all degrees and orders, in particular near orders of resonant geopotential coefficients. In addition, there is high-frequent aliasing of the geopotential coefficients when temporal gravity field solutions are computed. Therefore algorithms for smoothing and destriping are necessary when the spherical harmonic coefficients are converted into EWH variations. Details on this procedure are given by Wahr et al. (1998) and Chambers (2006). The EWH grids used in our study of the water mass variations in Central Europe have been smoothed with a Gaussian filter with a half-width of 400 km. A long-term average over 2003-2005 has been removed from the spherical harmonic coefficients. Note, that the MRR approach does not require additional smoothing and destriping since as mentioned before the scaling functions act as low-pass filters.

Gridded EWHs from the MRR approach and the spherical harmonic solutions are averaged over the area of the seven river basins and converted into units of km^3 water, i.e., the total variation of equivalent water in the studied area with respect to a long-term mean. In the case of the MRR this mean field is assumed to be the gravity field GGM01C complete to spherical harmonic degree 120.

3 Atmospheric Moisture Budget and River Runoff

The integrated GRACE EWHs are compared with water storage variations computed from independent atmospheric and hydrological data sets. The balance of inflow and outflow of water with respect to the examined area A is derived from the net effect of precipitation and evaporation $(P-E)_A(t)$ from the convergence of vertically integrated water vapor fluxes reduced by river discharge $R_A(t)$ from gauge registrations. The water balance equation reads

$$\Delta S_A(t) = (P-E)_A(t) - R_A(t), \tag{3}$$

where $\Delta S_A(t)$ denotes the storage change in the area.

For each time step precipitation minus evaporation is computed from the atmospheric moisture budget:

$$P - E = -\frac{\partial W}{\partial t} + \boldsymbol{\nabla}^T \boldsymbol{Q} \tag{4}$$

(Oki et al., 1995; Cullather et al., 1998), wherein W is precipitable water and $\boldsymbol{Q}$ is the vertically integrated water vapor flux. The first term on the right hand side is negligible on monthly and annual timescales (Cullather et al., 2000; Serreze et al., 2002), the second term is calculated from six hour atmospheric reanalysis products from the National Centers for Environmental Prediction/National Center for Atmospheric Research (NCEP/NCAR) (Kalnay et al., 1996) between 2002 and 2007 following equation

$$\boldsymbol{Q} = \int_{p_{sfc}}^{p_{top}} \rho\, \boldsymbol{v}\, \frac{\mathrm{d}p}{g} = \left[\int_{p_{sfc}}^{p_{top}} \rho\, u\, \frac{\mathrm{d}p}{g}; \int_{p_{sfc}}^{p_{top}} \rho\, v\, \frac{\mathrm{d}p}{g} \right]^T, \tag{5}$$

wherein g is the (mean) gravitational acceleration, p_{sfc} stands for the surface pressure, and p_{top} denotes the pressure at the highest atmospheric level. Our practical computations extend to $p_{top} = 300$ hPa since the specific humidity ρ is considered to be negligible above (i.e., no values for ρ are provided by NCEP/NCAR for pressure layers with $p < 300$ hPa). The horizontal wind vector $\boldsymbol{v} = [v, u]^T$ comprehends the two components v and u; the meridional component v is defined positive northwards, the zonal component u is defined positive eastwards.

The net inflow of water into the area A follows from

$$(P-E)_A = \int_A (P-E)\,\mathrm{d}A = \int_A \boldsymbol{\nabla}^T \boldsymbol{Q}\,\mathrm{d}A \tag{6}$$

$$= \oint_L \boldsymbol{Q}^T \boldsymbol{n}\,\mathrm{d}L. \tag{7}$$

In this equation the flux convergence is interpreted as line integral of the vertically integrated moisture transport along the boundary curve L of the area (dashed curve in Fig. 1, right) according to Gauss' Theorem; $\boldsymbol{n}$ is the unit normal to L. The total discharge from the area is calculated from gauge data of seven stations (black circles in Fig. 1, right) closest to the mouths of the rivers in the examined area.

We assume that the observations of those seven stations represent the net loss of water from the entire area. Therefore no further upstream gauges along the rivers are considered.

The gauge records were provided by the Global Runoff Data Centre (GRDC). Time series for the net inflow and outflow are shown in Fig. 2. The units of both $(P-E)_A$ and river discharge are derivatives with respect to time (km^3/month). Consequently the values have to be subtracted from each other and integrated in order to assess the instantaneous amount of water with respect to the initial water content $S_A(t_0)$ in the examined area for each time step:

$$S_A(t) = S_A(t_0) + \int_{t_0}^{t} (P-E)_A(\tau) - R_A(\tau) \, \mathrm{d}\tau. \tag{8}$$

Since the initial water content is unknown, the time series reflects residual variations of water mass in the area, i.e., the curve can be arbitrarily shifted along the ordinate.

FIGURE 2 HERE

4 Results

The results of the equivalent water mass variations in Central Europe from the three GRACE solutions and the independent atmospheric and hydrological data are displayed in Fig. 3 for the period between August 2002 and December 2006. The uncertainty of the GRACE EWHs is in the order of 1-2 cm (cf. Section 1). According to the law of error propagation, the accuracy of the storage variations of total water is limited to approximately 15-30 km^3 for the investigated area of $1.46 \cdot 10^6$ km^2.

As stated before the monthly fields of GFZ and CSR for June 2003 and January 2004 are missing. Between August and November 2004 when GRACE was almost in a repeat orbit GFZ and CSR provide constrained solutions. The resulting signal of the MRR is close to zero during this period and has been edited out of the data set.

FIGURE 3 HERE

The water mass variations $S_A(t)$ from the atmospheric moisture budget and river discharge agree remarkably well with the characteristics of the GRACE solutions. Correlation coefficients and root mean square (RMS) differences between the various curves are provided in Table 1. Between October and December 2002 and between May and August 2003 the result of the MRR approach shows better agreement with the independent data than the mass variations from the spherical harmonic solutions. We believe that one reason for this promising result is the regularization strategy which we apply to the regional data sets; see Schmidt et al. (2007). On the other hand the spherical harmonic solutions agree better with the atmospheric and hydrological data during the first half of 2005. This might be explained by increased scattering of the analyzed GRACE observations $\Delta V_{1,2}$ during this period. Even though there is an almost perfect agreement of the GFZ and CSR curves with $S_A(t)$ during autumn 2003 and (especially in the case of GFZ) during summer and autumn 2005, the phases of the storage variations from the spherical harmonic GRACE solutions and $S_A(t)$ are shifted during the rest of the time. The reason for this time lag between the curves is so far unexplained. Maximum agreement with GFZ and CSR would be reached if $S_A(t)$ was shifted about -30 days. Then the correlation coefficients would amount to 0.96 (GFZ) and 0.94 (CSR); respective RMS differences would decrease to 27.2 and 28.8 km^3.

TABLE 1 HERE

Large differences from year to year disallow an identification of a clear annual cycle in the curves. Obviously the underlying water storage changes are far from an annual behaviour due to changing meteorological conditions. Some specific features of the time series can be related to particular weather situations (Fig. 3). In the second half of 2002 Central Europe was affected by heavy rainfall which led to a rise of the Danube level up to 10 m above normal and caused devastating flooding of the Elbe from mid-August (Waple and Lawrimore, 2003). The water sojourned in the respective basins for a few month before the discharge peaks in November (Fig. 2). Especially the alpine region where most of the investigated rivers rise, experienced precipitation well above average in October and November. The strong rainfall in the Alps and the remaining floodwater resulted in anomalous high values of water storage. The increase of water mass between September and December 2002 is clearly visible in both the GRACE time series and the independent computations.

In summer 2003 Central Europe suffered a severe heat wave, which caused rivers to drop to record low levels. Between June and August the mean surface temperature was about 2.5°C above normal while the total precipitation was below average in the studied region (Levinson and Waple, 2004). The resulting drought is reflected by the GRACE observations (Andersen et al., 2005): All time series indicate a loss of approximately 150 km^3 of equivalent water from May to September 2003. Apart from a rather rainy summer season in some western areas the year 2004 featured normal weather patterns with average precipitation in most parts of Central Europe (Levinson, 2005). Therefore 2004 can be seen as a good reference to which exceptional patterns in other years might be compared. This is corroborated by analyses of $S_A(t)$ in earlier years without significant extreme events (e.g. 1996, 2000) in which the water storage variations did not exceed -100 and 100 km^3.

In the northern regions of the investigated area the year 2005 started with excess precipitation and deep winterly conditions that lasted until March. The period between July and August was characterized by ample rainfall. In August the precipitation exceeded the long term average by approximately 500% in the Danube basin which caused a severe flooding (Shein, 2006) (cf. Fig. 2). The increase of water mass during those two months is especially evident in the GRACE time series from GFZ and in the curve from atmospheric and hydrological data. Both curves conincide almost perfectly during this period. In November and December 2005 temperatures fell below average and by mid-November heavy snowfall affected the western regions.

The winter season 2005/2006 was characterized by ample snowfall which reached a record level in Germany during February (Arguez, 2007). In many parts of Central Europe precipitation was significantly above average during April, which caused - in combination with the melting snow - floodings at Elbe and Donau that even exceeded the 2002 summer records. With the exception of August which was quite wet, the period between June and September 2006 was anomalously dry with only 20-50% of normal rainfall in most areas. In Germany no month was warmer than July 2006 since the beginning of temperature registrations in 1900. In contrast, no August since 25 years was colder than August 2006. Those extremes left their fingerprints in the time series (especially in the curves of GFZ and the atmospheric and hydrological data) where the rapid decrease of water mass during summer is interrupted by a step in August. However the total water mass in the basins during August from $S_A(t)$ is significantly larger than observed by GRACE.

Expectedly, occasional discrepancies between the observations and the atmospheric and hydrological data are visible over the entire time span. On the one hand, the NCEP/NCAR and GRDC data sets are not free from errors, on the other hand mass variations computed from GRACE observations cannot be viewed as perfect representations of water storage changes either. The interpretability of the results in terms of water mass variations is limited due to significant discrepancies between the results from different analysis strategies as well as errors in the observation data and in the models and algorithms applied for de-aliasing and filtering. Furthermore the GRACE observations are influenced by geophysical processes apart from continental hydrology whose effects are widely unknown and by large-scale mass variations in adjacent areas. But nevertheless GRACE is a valuable contribution to the study and quantification of hydrological mass variations and snow accumulations which is demonstrated by the overall good agreement between the time series with respect to their shapes and amplitudes.

5 Acknowledgments

We thank H. Schuh and R. Gross for their quick and constructive reviews of the manuscript. This work is partially supported by NASA (NNG04GF01G and NNG04GN19G), and by NSF's CMG Program (EAR0327633). We acknowledge the NASA/DLR

GRACE project for the GRACE data products (distributed by JPL PODAAC) and S. Bettadpur for providing precise GRACE orbits with finer temporal resolutions for our data processing. GRACE spherical harmonic solutions were processed by D. Chambers, supported by the NASA Earth Science REASoN GRACE Project. NCEP/NCAR reanalysis data was provided by the NOAA/OAR/ESRL PSD, Boulder, Colorado, USA. River gauge data was derived from the Global Runoff Data Centre (GRDC), D-56002 Koblenz, Germany.

References

Andersen, O., S. Seneviratne, J. Hinderer, and P. Viterbo (2005). GRACE-derived terrestrial water storage depletion associated with the 2003 European heat wave. *Geophys. Res. Lett.*, *32*, L18405, doi:10.1029/2005GL023574.

Arguez, A. (Ed.) (2007). *State of the Climate in 2006*. Bull. Amer. Meteor. Soc., 88(6), S1-S135.

Chambers, D. (2006). Evaluation of new GRACE time-variable gravity data over the ocean. *Geophys. Res. Lett.*, *33*, LI7603, doi: 10.1029/2005GL022382

Cullather, R., D. Bromwich, and M. van Woert (1998). Spatial and temporal variability of Antarctic precipitation from atmospheric methods. *J Climate*, *11*, 334-367

Cullather, R., D. Bromwich, and M. Serreze (2000). The atmospheric hydrologic cycle over the Arctic basin from reanalyses. Part I: Comparison with observations and previous studies. *J Climate*, *13*, 923-937

Farrell, W.E. (1972). Deformation of the Earth by surface loads. *Rev. Geophys. Space Phys.*, *10*, 761-797

Flechtner, F. (2003). AOD1B Product Description Document. GRACE Project Documentation, JPL 327-750, Rev. 1.0, JPL Pasadena, CA.

Han, S., C.K. Shum, C. Jekeli (2006). Precise estimation of in situ geopotential differences from GRACE low-low satellite-to-satellite tracking and accelerometry data. *J. Geophy. Res.*, *111*, B4411, doi:10.1029/2005JB003719.

Kalnay, E., M. Kanamitsu, R. Kistler, et al. (1996). The NCEP/NCAR 40-year reanalysis project. *Bull. Amer. Meteor. Soc.*, *77*, 437-471.

Levinson, D. (Ed.) (2005). *State of the Climate in 2004*. Bull. Amer. Meteor. Soc., 86(6), S1-S86.

Levinson, D., and A. Waple (Eds.) (2004). *State of the Climate in 2003*. Bull. Amer. Meteor. Soc., 85(6), S1-S72.

Oki, T., K. Musiake, H. Matsuyama, and K. Masuda (1995). Global atmospheric water balance and runoff from large river basins. *Hydrological Proc.*, *9*, 655-678

Schmidt, M., M. Fengler, T. Mayer-Gürr, A. Eicker, J. Kusche, L. Sánchez, and S.-C. Han (2007). Regional Gravity Modelling in Terms of Spherical Base Functions. *J Geod*, *81*, pp 17-38, doi: 10.1007/s00190-006-0101-5

Schmidt, M., F. Seitz, and C.K. Shum (est. 2008). Regional 4-D hydrological mass variations from GRACE, atmospheric flux convergence and river gauge data.

Submitted to *J. Geophy. Res.*.

Schmidt, R., P. Schwintzer, F. Flechtner, C. Reigber, A. Güntner, P. Döll, G. Ramillien, A. Cazenave, S. Petrovic, H. Jochmann, and J. Wünsch (2006). GRACE observations of changes in continental water storage. *Global and Planetary Change*, *50*, 112-126.

Serreze, M., D. Bromwich, M. Clark, A. Etringer, T. Zhang, and R. Lammers (2002). Large-scale hydro-climatology of the terrestrial Arctic drainage system. *J. Geophy. Res.*, *107*, 8160, doi:10.1029/2001JD000919.

Shein, K. (Ed.) (2006). *State of the Climate in 2005*. Bull. Amer. Meteor. Soc., *87(6)*, S1-S102.

Swenson, S., J. Wahr, and P. Milly (2003). Estimated accuracies of regional water storage variations inferred from the Gravity Recovery and Climate Experiment (GRACE). *Water Resources Research*, *39(8)*, doi:10.1029/2002WR001736.

Swenson, S., P. Yeh, J. Wahr, and J. Famiglietti (2006). A comparison of terrestrial water storage variations from GRACE with in situ measurements from Illinois. *Geophys. Res. Lett.*, *33*, L16401, doi:10.1029/2006GL026962.

Tapley, B.D., S. Bettadpur, J. Ries, P. Thompson, and W. Watkins (2004). GRACE measurements of mass variability in the Earth system. *Science*, *305*, 503-505.

Wagner, C., D. McAdoo, J. Klokočník, and J. Kostelecký (2006). Degradation of Geopotential Recovery from Short Repeat-Cycle Orbits: Application to GRACE Monthly Fields. *J. Geodesy*, *80*, 94-103.

Wahr, J., M. Molenaar, and F. Bryan (1998). Time-variability of the Earth's gravity field: Hydrological and oceanic effects and their possible detection using GRACE. *J. Geophy. Res.*, *103*, 32205-30229.

Wahr, J., S. Swenson, and I. Velicogna (2006). Accuracy of GRACE mass estimates. *Geophys. Res. Lett.*, *33*, L06401, doi:10.1029/2005GL025305.

Waple, A., and J. Lawrimore (Eds.) (2003). *State of the Climate in 2002*. Bull. Amer. Meteor. Soc., 84(6), S1-S68.

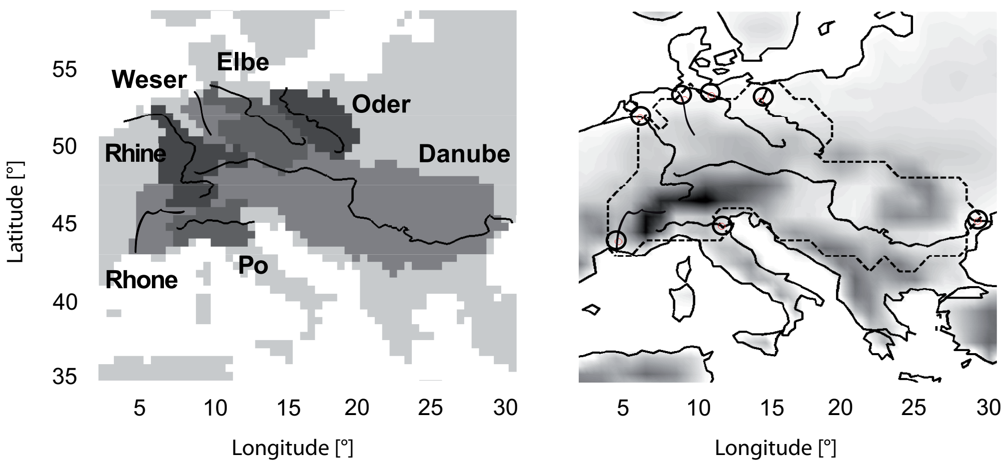

Fig. 1. (left) The area investigated in this study is composed of the seven largest river basins in Central Europe. (right) The dashed line is the boundary of the area, black circles show locations of river gauges used for discharge information.

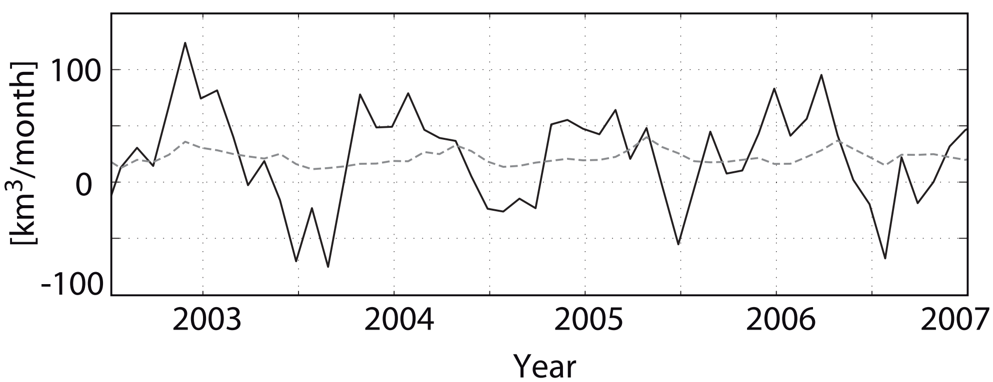

Fig. 2. Net inflow from the atmospheric moisture budget (solid) and outflow from river gauge data (dashed) for the area of the seven Central European river basins.

Table 1

Correlation coefficients and RMS differences between the various time series of water storage variation from GRACE solutions (MRR, GFZ, CSR) and from atmospheric reanalyses and river gauges ($S_A(t)$).

	Correlation coefficient	RMS difference [km^3]
MRR - GFZ	0.89	34.0
MRR - CSR	0.91	31.4
GFZ - CSR	0.97	16.3
MRR - $S_A(t)$	0.90	36.2
GFZ - $S_A(t)$	0.89	34.4
CSR - $S_A(t)$	0.86	38.9

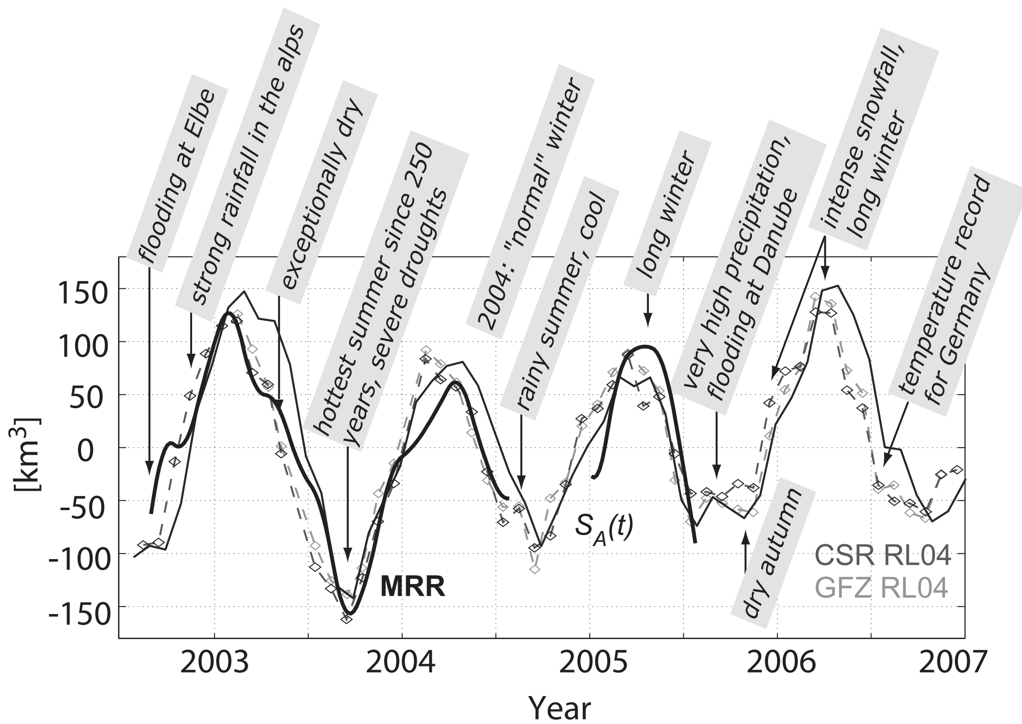

Fig. 3. Mass variations in the investigated area in units of km^3 of equivalent water from the 4-D multi-resolution representation (solid bold) and two solutions based on global spherical harmonics from GFZ (dashed gray) and CSR (dashed black). The thin black curve shows the independent results from atmospheric and hydrological data.